Jiang *et al. Chin. J. Mech. Eng.* (2018) 31:21
https://doi.org/10.1186/s10033-018-0227-4

Chinese Journal of Mechanical Engineering

ORIGINAL ARTICLE

Open Access

Leakage and Stiffness Characteristics of Bionic Cluster Spiral Groove Dry Gas Seal

Jin-Bo Jiang, Xu-Dong Peng*, Ji-Yun Li and Yuan Chen

Abstract

Spiral groove dry gas seal (S-DGS), the most widely used DGS in the world, encounters the problem of high leakage rate and inferior film stability when used in high-speed machinery equipment, which could not be well solved by optimization of geometrical parameters and molded line of spiral groove. A new type of bionic cluster spiral groove DGS (CS-DGS) is proved to have superior film stability than S-DGS at the condition of high-speed and low-pressure numerically. A bionic CS-DGS is experimentally investigated and compared with common S-DGS in order to provide evidence for theoretical study. The film thickness and leakage rate of both bionic spiral groove and common spiral groove DGS are measured and compared with each other and with theoretical values under different closing force at the condition of static pressure, high-speed and low-pressure, and the film stiffness and stiffness-leakage ratio of these two face seals are derived by the relationship between closing force and film thickness at the steady state. Experimental results agree well with the theory that the leakage and stiffness of bionic CS-DGS are superior to that of common S-DGS under the condition of high-speed and low-pressure, with the decreasing amplitude of 20% to 40% and the growth amplitude of 20%, respectively. The opening performance and stiffness characteristics of bionic CS-DGS are inferior to that of common S-DGS when rotation speed equals to 0 r/min. The proposed research provides a new method to measure the axis film stiffness of DGS, and validates the superior performance of bionic CS-DGS at the condition of high-speed and low-pressure experimentally.

Keywords: Bionic cluster spiral groove, Film stiffness, Dry gas seal, Leakage rate

1 Introduction

Dry gas seals with unidirectional spiral groove (S-DGS) have encountered numerous applications in medium and high speed rotating equipment because of their low friction, long life time, such as centrifugal compressors, pumps and blowers [1–6]. However, the abrupt failure of S-DGS occurs from time to time when used in high speed machinery with big vibration for the weak capacity of resisting disturbance of gas film between the two faces. Strict environmental protection laws require efficient sealing systems for preventing release of the poisonous and harmful fluids into atmosphere, which bring forward higher request for the sealing performance of S-DGS. Leakage rate and film stiffness are the two key sealing performance parameters of dry gas seal. The purpose of a seal is to prevent leakage; hence, the leakage path should be as small as possible, and the leakage rate should be as low as possible. The axial film stiffness is used to characterize the capacity of resisting disturbance of gas film. The higher of film stiffness, the stronger capacity of resisting disturbance of gas film; hence, it is of cardinal importance to enhance the stiffness of gas films to minimize vibration due to external excitations. The separation gap between the frictional surfaces deeply influence the leakage rate and film stiffness, which created by the opening force, and should be neither too large nor too small: if the film gap is too large, the process fluid leaks across the faces and lead to the large leakage rate and small film stiffness; and if too small, excessive wear is likely to occur [7].

In order to maximize the film stiffness of dry gas seal, and keep a low leakage rate at the same time, a great deal of numerical and experimental study on groove structure

*Correspondence: xdpeng@126.com
Engineering Research Center of Process Equipment and Its Re-manufacturing of Ministry of Education, Zhejiang University of Technology, Hangzhou 310014, China

and parameter optimization of DGS under varying operation conditions have been carried out. The effect of geometry parameters of groove, such as spiral angle, groove-dam ratio and groove depth, on the performance of a S-DGS, such as opening force, film stiffness, leakage rate and stiffness-leakage ratio, are numerically analyzed by Zirkelback et al. [8], Liu et al. [9], Peng et al. [10]. The optimum structural parameters of groove with different objective functions in different operating conditions are presented. In recent years, the effect of groove structural optimization on performance improvement of DGS has attracted more and more researchers' attention because the limitation of performance enhancement by optimum design of groove geometry parameters of S-DGS simply. Recently, a parametric study and performance evaluation of typical bidirectional dry gas seals with modified surface were presented by Su et al. [11, 12] and Blasiaka and Zahorulko [13]. Hashimoto and Ochiai [14–16] presented an entirely new optimum design methodology, in which the groove geometry can be flexibly changed by using the spline function, to maximize the stiffness of gas films for grooved thrust bearings. The film stiffness and load-capacity of the optimized bearing are higher than that of common spiral groove bearing and herringbone bearing, which were both theoretically and experimentally verified. The sealing performance of the spiral groove DGS with an inner annular groove (AS-DGS) [17] was numerically analyzed by Peng et al. [18], which was invented by Flowserve Corporation. The results show that the opening force and film stiffness of AS-DGS is larger than that of the common S-DGS at the condition of low-speed and high-pressure, while the leakage is a little larger. Dresser-Rand Corporation presented a patented pattern of short grooves in combination with the longer grooves to provide excellent lift-off effect and optimum gas film stiffness at low speed as well as high speed. During operation, the short grooves could create obvious high pressure to separate the mating rings at slow speed, while the longer grooves contribute to creating a stable gas film between the two rings at high speed. The uni-directional V groove with the combined radial-circumferential tapered groove bottom [19], which was invented by Burgmann Corporation, causes a reduction in the opening force and leakage rate. Despite that there are only few researchers pay attention to the experiment of the sealing performance test of DGS, most of the researchers only focus on the numerical simulation and analysis of groove structure and geometry parameters optimization as the subject to improve the gas film stiffness and reduce the fluid leakage of DGS.

Jiang et al. [20, 21] introduces a new type of bionic cluster spiral groove dry gas seal (CS-DGS) based on the coupling bionic theory, and presents the numerical study on the influence of groove geometry parameters on the sealing performance, such as opening force, axial film stiffness and seal leakage. The results shows that the sealing performance and operation stability of bionic CS-DGS are much better compared to common unidirectional S-DGS at high speed.

The aim of this study is to investigate the leakage and stiffness characteristics of a bionic cluster spiral groove DGS experimentally which could provide evidence for the theoretical study. The film thickness and leakage rate of CS-DGS and S-DGS were measured and the closing force was calculated at the condition of static pressure and high-speed, and the measured data were compared with the theoretical results. The relationship between film stiffness and film thickness was derived from the relationship between opening force and film thickness. The experimental results could provide a reference for the design and model selection of CS-DGS in engineering.

2 Experiment

2.1 Experimental Apparatus

A schematic description of a test rig used in the present experiments is shown in Figure 1. It is composed of a power-driven system, a pressurized seal gas supply and regulation system, two external pressurized seals and a computerized data acquisition system. There are two face seals in the seal chamber, the right one is the grooved face seal used for testing, and the left one is the auxiliary seal which used to prevent the seal leakage to the side of bearing housing. The test smooth rotor ring is supported by a metallic holder on the axle sleeve of the shaft, which is driven by a motor whose rotation speed is controlled by a frequency converter. The shaft speed varies from 0 to 10000 r/min. The grooved ring (stationary ring) is mounted in the seal chamber and can freely move in the axial direction adjusted by the three uniformly distributed micro meters which are fixed to the housing. In order to measure the film thickness and leakage rate, a sensor holder is fixed on the test stationary ring. An eddy current displacement sensor is installed on the holder by thread and a stainless steel sheet is fixed on the test rotor by super glue. The on-line measurement of gas film thickness is carried out by measuring the displacement change between the eddy current sensor and the sheet during testing. The leaking gas goes out from the leakage rate measurement hold on the sensor holder, connected to leakage rate sensor, a digital MEMS gas mass flow meter, through pipe. Pressurized seal gas provided by a low pressure air compressor flows into the seal chamber after filtered (filter precision is less than 1 μm) and dehumidified by tertiary filters, and the pressure of which is adjusted by a pressure value and measured by a pressure sensor. All the data (including the data from the pressure

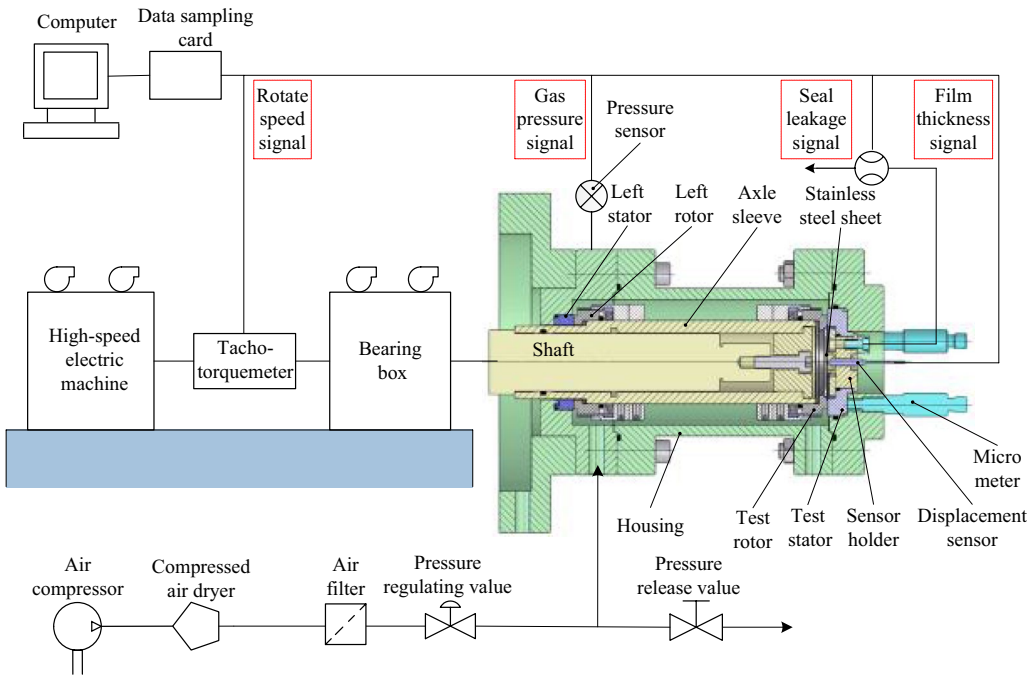

Figure 1 Schematic description of test rig

sensor, the speed control system, the eddy current sensor and the gas mass flow meter) collected from the sensors are fed into a data acquisition system and interfaced with a computer.

In order to measure the film thickness and leakage rate, a sensor holder is fixed on the test stationary ring. An eddy current displacement sensor is installed on the holder by thread and a stainless steel sheet is fixed on the test rotor by super glue. The on-line measurement of gas film thickness is carried out by measuring the displacement change between the eddy current sensor and the sheet during testing. The leaking gas goes out from the leakage rate measurement hold on the sensor holder, connected to leakage rate sensor, a digital MEMS gas mass flow meter, through pipe. Pressurized seal gas provided by a low pressure air compressor flows into the seal chamber after filtered (filter precision is less than 1 μm) and dehumidified by tertiary filters, and the pressure of which is adjusted by a pressure value and measured by a pressure sensor. All the data (including the data from the pressure sensor, the speed control system, the eddy current sensor and the gas mass flow meter) collected from the sensors are fed into a data acquisition system and interfaced with a computer.

Some special measures had been taken to improve the measurement accuracy of leakage rate. The collector of leakage from the mating surface and its' auxiliary structure for preventing leakage through other paths except the path of leaking gas collector are shown in Figure 2. The O rings are used to prevent the leakage between stator ring and sensor holder, and between bolt and sensor holder respectively. The thread seal taper is used to prevent the leakage between displacement sensor and sensor holder.

The high seal pressure p_o is provided at the outside of the seal rings and low pressure p_i at the inside as shown in Figure 3, which provides the gas film opening force F_o and static pressure closing force F_{sta}, respectively. The closing force F_c consists of the static pressure closing force F_{sta} and the spring force F_{sp}. The spring force F_{sp} could be adjusted by the micro meter without disassembling the test seal, for the spring camber would be

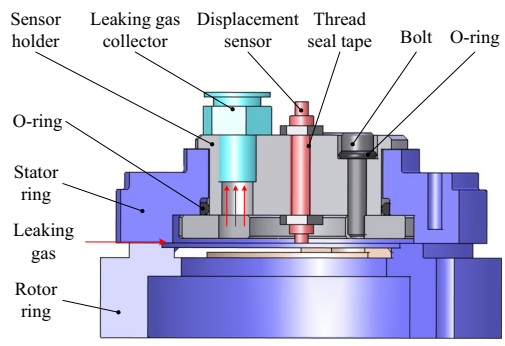

Figure 2 Leaking gas collector and its auxiliary structure

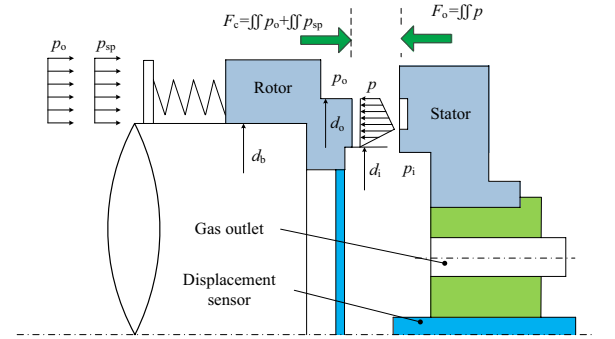

Figure 3 Illustration of the forces applied on the rotor ring

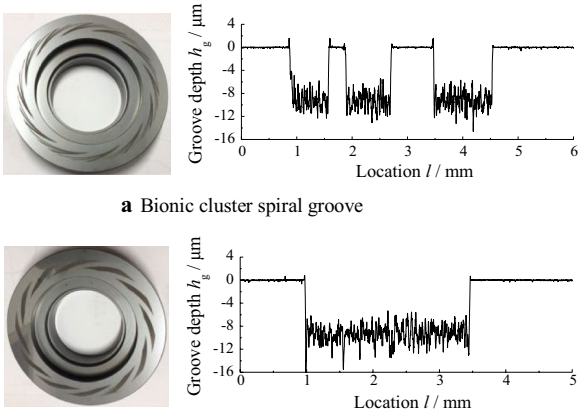

Figure 4 Image and profile of two different types of grooves

changed when adjusting the micro meter, the accuracy of adjustment of which is 0.01 mm. Here, the spring force F_{sp} is expressed as

$$F_{sp} = 0.25Nk\pi\left(d_o^2 - d_i^2\right) \triangle x, \quad (1)$$

and the static closing force F_{sta} is obtained as

$$F_{sta} = 0.25\pi\left(d_o^2 - d_b^2\right)p_o + 0.25\pi\left(d_b^2 - d_i^2\right)p_i, \quad (2)$$

where N is the number of spring, k is the average spring stiffness, Δx is the spring camber, and d_o, d_i, d_b are the outer, inner and balanced diameter of the seal face, respectively.

When the seal is in steady running state at a constant seal gap, the closing force F_c generated by the spring and pressurized seal gas would balance with the opening force F_o, the following equation is obtained:

$$F_o = F_c = F_{sp} + F_{sta} \quad (3)$$

2.2 Specimen Preparation

The specimens are made in pairs. The plain, rotating ring with an I.D. of 59 mm, O.D. of 73 mm is made of carbon because of its superior wear and corrosion properties. Silicon carbide has been chosen as the material of stationary ring for its high hardness and thermal conductivity, low coefficient of thermal expansion and good compatibility with carbon [22]. The stationary ring is larger in size and textured with two different types of grooves: spiral groove and bionic cluster spiral groove which is made for comparison purpose, and the friction surfaces are polished. Figure 4 shows the photographs of the stationary rings textured with bionic cluster spiral groove (a) and spiral groove (b) where the textured areas appear as darker matt surface, and the 2D profile of grooves marked by the Optical Fiber Laser Marking machine, which are obtained by Dektakxt Stylus Profiler. The groove depth is controlled by the laser power, scanning speed and interval of the laser beam. In this experiment, when the laser power set to 30% of its full capacity, scanning speed of 100 mm/s and scanning internal of 0.05, the measured groove depth is about 9 μm. Roughness of untextured region is $Ra = 0.05$ μm, and the roughness of the bottom of grooves is $Ra = 0.8$ μm.

The configuration of the bionic cluster spiral groove is illustrated in Figure 5 and the geometrical parameters are

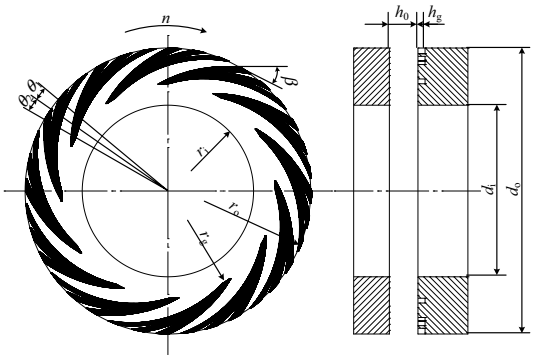

Figure 5 Schematic diagram of the grooved face of cluster spiral groove dry gas seal

Table 1 Specifications for cluster spiral groove seal face

Item	Value
Outside radius r_o (mm)	36.5
Inside radius r_i (mm)	29.5
Balance radius r_b (mm)	32.5
Groove number N_g	12
Spiral angle β (°)	15
Groove-dam ratio a_g	1.5
Groove-land ratio δ	1.0

listed in Table 1, where r_i, r_o and r_g are the inner, outer and groove-dam boundary radii, respectively; β is the spiral angle, θ_1 and θ_2 are the circumferential angle of groove region and land region in one cycle, h_g is the groove depth and h_0 is the film thickness in the dam region, n is the rotational speed of the rotating ring. To characterize the ratio of groove region in the circumferential direction, the groove-land ratio δ is defined as follows:

$$\delta = \frac{\theta_1}{\theta_2}, \tag{4}$$

To characterize the ratio of groove region in the radial direction, the groove-dam ratio α_g is defined as follows:

$$\alpha_g = \frac{r_o - r_g}{r_o - r_i}. \tag{5}$$

To compare the bionic cluster spiral groove with conventional spiral groove under the same baseline, the groove number, spiral angle, groove depth, groove-land ratio and groove-dam ratio of these two types of groove have the same value.

2.3 Experimental Procedure

The experimental procedure for investigation of leakage and stiffness characteristics of bionic cluster spiral groove DGS and spiral groove DGS are provided as follows. Firstly, the rotating rings and stationary rings are cleaned in a bath ultrasonically with acetone for 5 min, the spring stiffness of the springs used is measured and eddy current sensor is calibrated before the experiment. Secondly, the stator and rotor specimens are installed in the holders, and the spring compression is measured. The desired gas pressure is set to 0.5 MPa and 0.4 MPa in the hydrostatic performance test and hydrodynamic performance test respectively; the speed of the motor is programmed to 8000 r/min in the dynamic pressure performance test. Spring force is changed by steps of 3 N, adjusted by the three uniformly distributed micro meters, and each force step is maintained for 1 min following the stabilization of the film thickness and leakage rate at a steady value. The test ends when a minimum film thickness of 1.5 μm is reached or if the leakage rate exceeds a value of 10 L/min. The gas pressure in the chamber under constant rotational speed and spring force is increased in a stepwise manner to examine the leakage and stiffness characteristics of these two types of DGSs at different gas pressure. In each step, the machine runs at a constant speed and gas pressure for 1 min. Each of the carbon rotating rings is used less than five times to ensure that the end faces are hardly worn. What's more, experiments for the same seal ring under the given conditions are repeated twice to guarantee the repeatability of the results. At the same time, the film thickness, leakage rate, gas pressure and rotational speed are monitored and recorded by a high-speed data acquisition system with a sampling rate of 1000 Hz. At last, the collected data are output to an ".xls" file for graphic presentation.

3 Results and Discussion

Theoretical analysis is also carried out to analyze the results. Based on the assumptions that fluid body forces are negligible, fluid viscous forces dominate over fluid inertia forces, the variation of pressure across the fluid film is negligibly small, and the fluid film thickness is much less than the width and length, the pressure distribution over a single period of grooves for Newtonian gas in laminar flow is obtained from the Reynolds equation [23]:

$$\frac{\partial}{r\partial\theta}\left(\frac{h^3}{\mu}\frac{\partial p^2}{r\partial\theta}\right) + \frac{\partial}{\partial r}\left(\frac{h^3}{\mu}\frac{\partial p^2}{\partial r}\right) = 12\omega\frac{\partial(ph)}{\partial\theta}, \tag{6}$$

where p is the local pressure, h is the local film thickness, μ is the viscosity, ω is the angular velocity.

The opening force F_o, leakage rate q, film stiffness k_z and stiffness-leakage ratio Γ are expressed as following equations:

$$F_o = \int_0^{2\pi}\int_{r_i}^{r_o} pr\mathrm{d}r\mathrm{d}\theta, \tag{7}$$

$$q = \frac{h^3 r}{12\mu p_i}\int_0^{2\pi}\frac{\partial p}{\partial r}p\mathrm{d}\theta, \tag{8}$$

$$k_z = \frac{\partial F_o}{\partial h}, \tag{9}$$

$$\Gamma = \frac{k_z}{q}. \tag{10}$$

Figure 6 shows the theoretical values of opening force and closing force of S-DGS and CS-DGS with increasing film thickness under seal pressure of 0.4 MPa and 0.5 MPa. As can be seen, when the rotational speed increased from 0 to 8000 r/min under seal pressure of 0.4 MPa and film thickness of 1 μm, the opening force of CS-DGS and S-DGS increased remarkably by 70% and 60%, respectively. In this case, the hydrodynamic effect generated by CS-DGS is much larger than that of S-DGS. Another important result shown in Figure 6 is that the seal faces of CS-DGS can be separated by a static seal pressure of 0.4 MPa under spring pressure of 0.04 MPa and 0.06 MPa and correspondingly the film thickness value are 4.7 μm and 1.6 μm. Moreover, the film thickness will increase with increasing rotational speed and decreasing spring pressure.

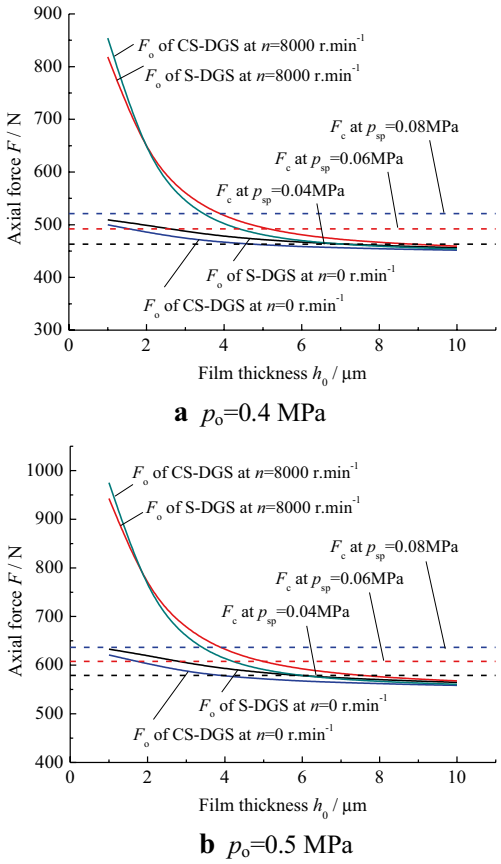

Figure 6 Theoretical results of opening force of S-DGS and CS-DGS with increasing clearance

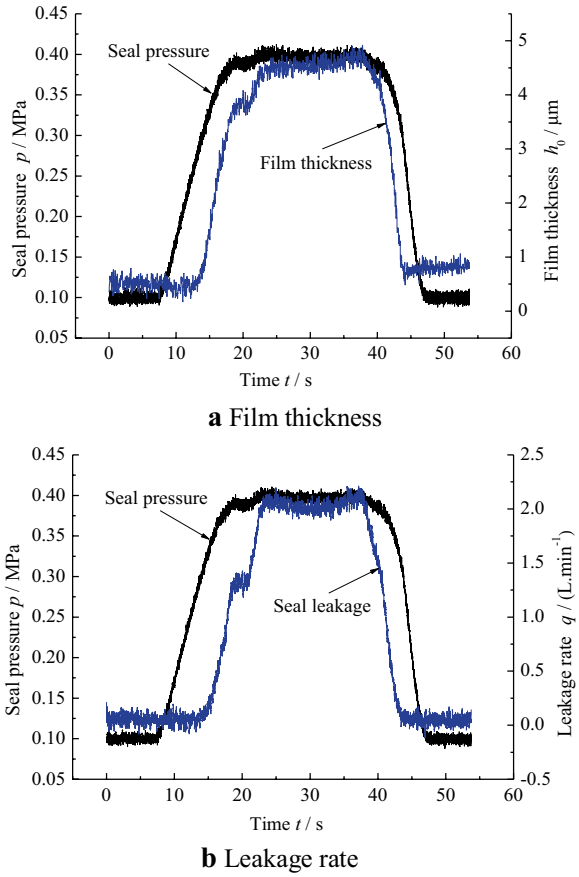

Figure 7 Seal pressure, leakage rate and film thickness curves vs time

3.1 Hydrostatic Characteristics Test

Figure 7 shows the variation tendency of the film thickness and leakage rate of CS-DGS with seal pressure increased from 0 up to 0.4 MPa, kept the pressure state for 30 s after both film thickness and leakage rate reached a steady state, and then down to 0 again during the experiment. It can be seen that when the seal pressure increased higher than 0.30 MPa, the seal faces open suddenly and the film thickness and leakage rate increase obviously. The seal faces maintain an open state with a film thickness of 4.5 μm and leakage rate of 2.1 L/min when the seal pressure reaches a steady value of 0.40 MPa.

The experimental results of opening force and leakage rate in different film thickness of CS-DGS are compared with that of the theoretical results obtained using the geometric parameters for the test bionic cluster spiral groove seal shown in Table 1, as shown in Figure 8. For the opening force, the agreement between experimental and theoretical results is good, with differences of less than 10% over the entire film thickness range. The experimental result of the leakage rate is about 30% larger than the theoretical value when film thickness is larger than 4 μm, while the measured experimental leakage rates are much larger than the theoretical predictions particularly when film thickness is lower than 3 μm.

Figure 9 presents the experimental results and fitted lines of opening force and leakage rate with increasing film thickness of S-DGS (solid line) and CS-DGS (dash line) under a seal pressure of 0.5 MPa. It can be seen from Figure 9 that the opening force of CS-DGS is about 4% lower than that of S-DGS, while the leakage rate of them two is almost equal. The relationship between fitted value of opening force and film thickness of CS-DGS and S-DGS can be expressed by the following equation, respectively:

$$F_o = 568.13h_0^{-0.0181}, \tag{11}$$

$$F_o = 591.87h_0^{-0.0317}. \tag{12}$$

Film stiffness and stiffness-leakage ratio of can be obtained according to Eqs. (11), (12), respectively.

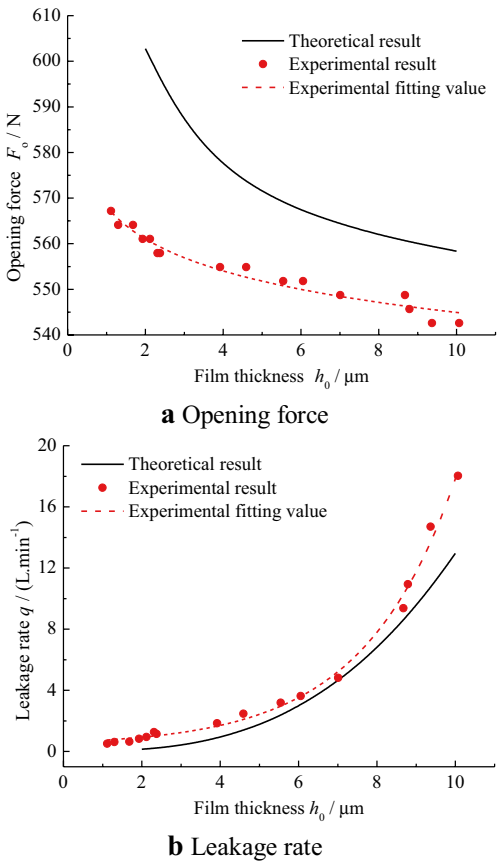

Figure 8 Comparison of the theoretical result and experimental result of the opening force and seal leakage of CS-DGS versus the film thickness

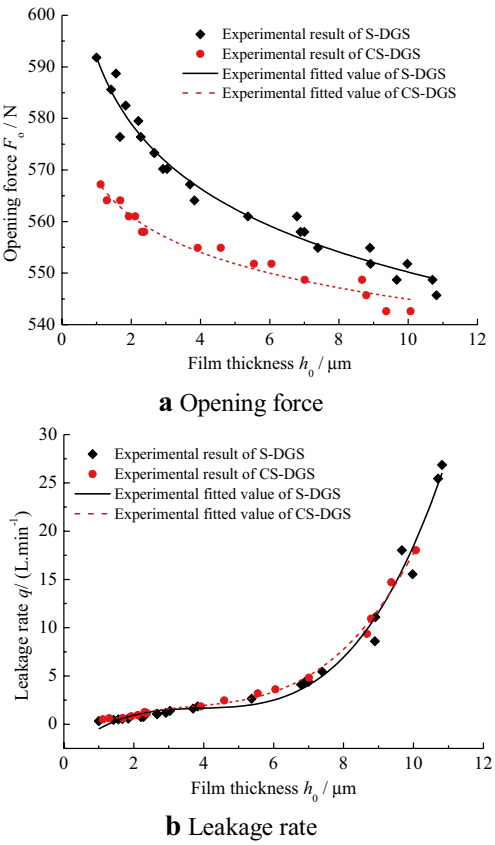

Figure 9 Comparison of the experimental result and fitted value of opening force and seal leakage of S-DGS and CS-DGS

Figure 10 shows the calculation results of film stiffness and stiffness-leakage ratio with increasing film thickness of S-DGS (solid line) and CS-DGS (dash line). Clearly, both the film stiffness and stiffness-leakage ratio of CS-DGS are lower than that of S-DGS over the entire film thickness range. The above experimental comparison results of sealing performance parameters with increasing film thickness between CS-DGS and S-DGS under a pressure of 0.5 MPa indicate that the opening characteristics and film stability of S-DGS are superior to that of CS-DGS under the condition of static seal pressure when rotation speed equals to 0 r/min.

3.2 Hydrodynamic Characteristics Test

In order to study the change of film thickness and leakage rate of CS-DGS as seal pressure and rotational speed change, the seal pressure and rotational speed are adjusted to from 0 to 0.4 MPa and from 0 to 8000 r/min, respectively. The variation tendency of film thickness and leakage rate of CS-DGS during the change of seal pressure and rotational speed is shown in Figure 11. As a first step, the seal pressure increased from 0 up to 0.4 MPa, and then the seal faces maintained an open state with a film thickness of 3.2 μm and leakage rate of 0.6 L/min when the seal pressure reached a steady value of 0.4 MPa. After that the rotational speed increased from 0 up to 8000 r/min at a time of 15 s after both film thickness and leakage rate reached a steady state, and then the seal faces operated with a film thickness of 6.0 μm and leakage rate of 2.2 L/min under a seal pressure of 0.4 MPa and a rotational speed of 8000 r/min. The fact of the remarkable increasing of film thickness when rotational speed increase from 0 to 8000 r/min illustrates that the bionic cluster spiral groove produces considerable hydrodynamic opening force to make the seal faces separate further, indicating that bionic spiral groove DGS could generate strong hydrodynamic effect in high speed.

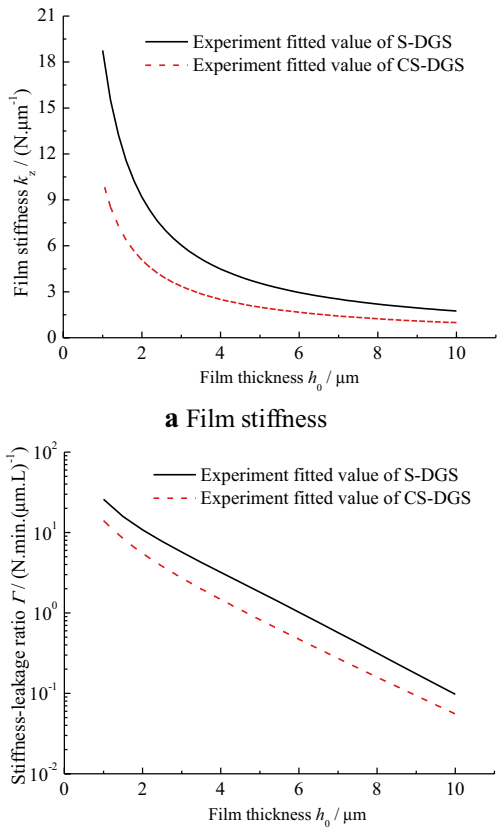

a Film stiffness

b Stiffness-leakage ratio

Figure 10 Comparison of experiment fitted value of film stiffness and stiffness-leakage ratio of S-DGS and CS-DGS

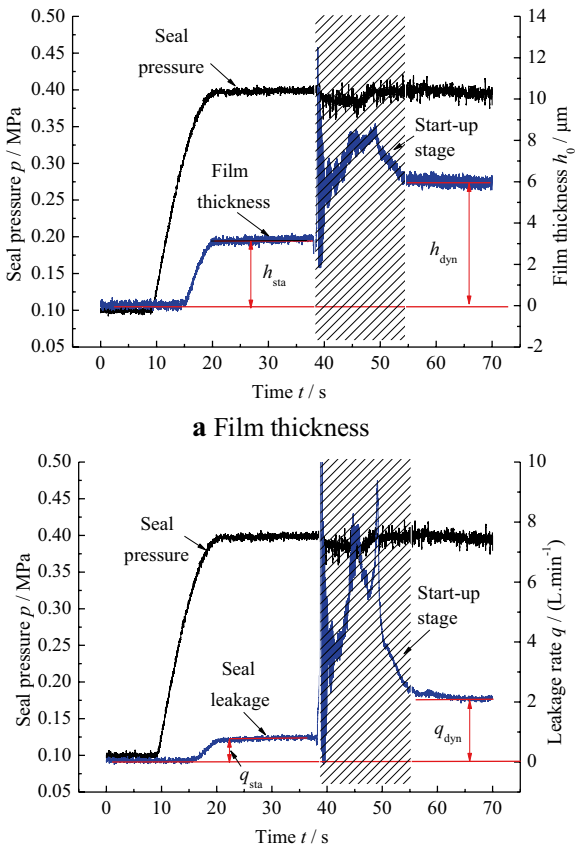

a Film thickness

b Leakage rate

Figure 11 Seal pressure, leakage and film thickness curves versus time

The experimental results of opening force and leakage rate in different film thickness of CS-DGS are compared with that of the theoretical results under the condition of $p_o = 0.4$ MPa and $n = 8000$ r/min, as shown in Figure 12. For opening force, the agreement between experimental and theoretical results is good when film thickness is larger than 4 μm, with differences of less than 10%. The influence of roughness of groove bottom on sealing performance gradually increases when film thickness is very small, which leads to the difference between experimental and theoretical results.

Figure 13 presents the experimental results and fitted lines of opening force and leakage rate with increasing film thickness of S-DGS (solid line) and CS-DGS (dashed line) under a seal pressure of 0.4 MPa and rotational speed of 8000 r/min. As can be seen the opening force of CS-DGS is very similar with that of S-DGS, especially when film thickness is smaller than 2 μm. Another important result shown in Figure 13 is that the leakage rate of CS-DGS is lower 20% to 40% than that of S-DGS when film thickness ranges from 2 μm to 5 μm, which indicates the excellent sealing performance of CS-DGS in high speed.

The relationship between fitted value of measured experimental opening force and film thickness of CS-DGS and S-DGS can be expressed by the following equations, respectively:

$$F_o = 481.85 h_0^{-0.0393}, \tag{13}$$

$$F_o = 485.87 h_0^{-0.0327}. \tag{14}$$

The film thickness and stiffness-leakage ratio obtained by calculating Eqs. (13), (14) with increasing film thickness of S-DGS (solid line) and CS-DGS (dashed line)

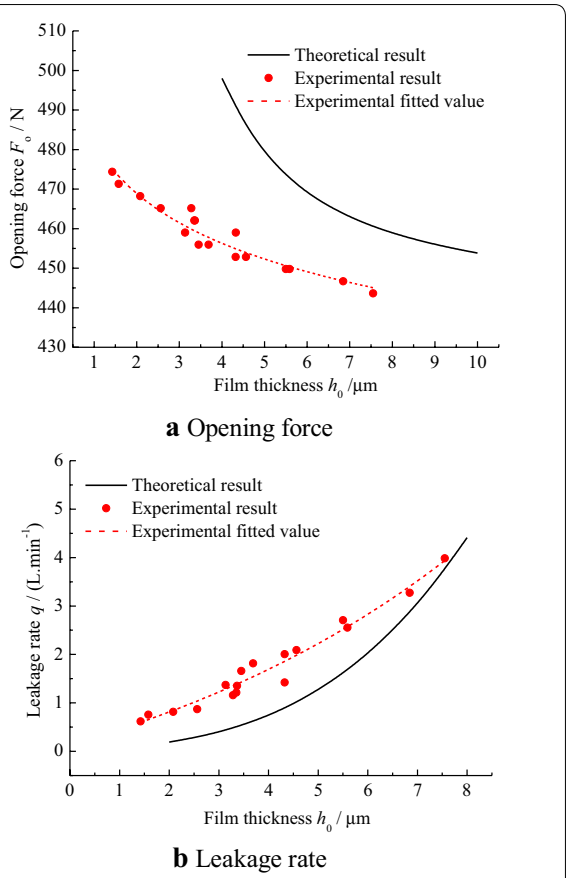

a Opening force

b Leakage rate

Figure 12 Comparison of the theoretical result and experimental result of the opening force and seal leakage of CS-DGS

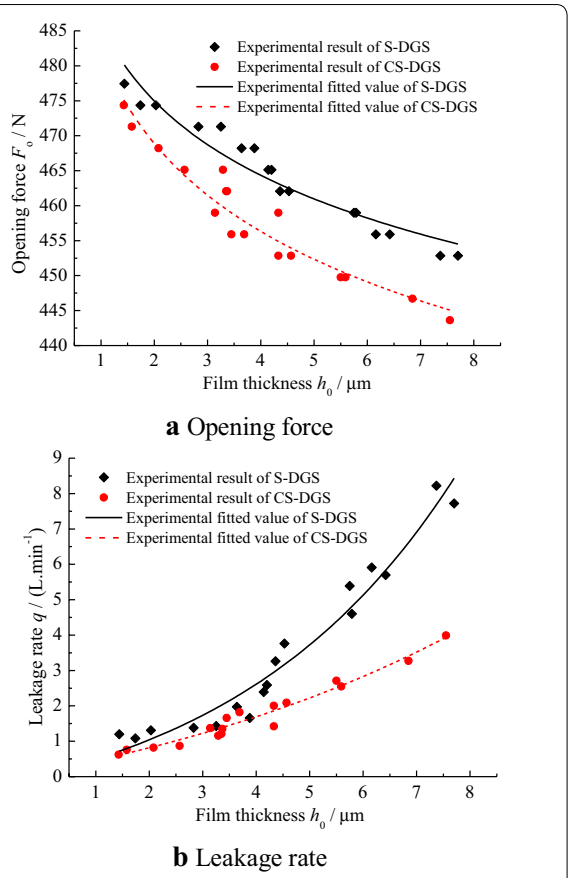

a Opening force

b Leakage rate

Figure 13 Comparison of the experimental result and fitted value of opening force and seal leakage of S-DGS and CS-DGS

are shown in Figure 14. Clearly, both the film stiffness and stiffness-leakage ratio of CS-DGS are much larger than that of S-DGS over the entire film thickness range. The film stiffness and stiffness-leakage ratio of CS-DGS are 20% and 60% higher than that of S-DGS respectively when film thickness is 3 μm. As mentioned above, the excellent film stability of CS-DGS at the condition of high-speed and low-pressure is due to the strong hydrodynamic effect generated by the bionic cluster spiral groove, which lead to the enough hydrodynamic force and maintain a stable fluid film between the two seal faces.

4 Conclusions

(1) A new method to measure axial gas film stiffness of dry gas seals experimentally is proposed. The experimental results of opening force and leakage rate of bionic CS-DGS agrees well with that of theoretical values when film thickness is larger than 4 μm.

(2) The opening performance and stiffness characteristics of bionic CS-DGS are inferior to that of common S-DGS when rotation speed equals to 0 r/min, which indicate that CS-DGS is not suitable for low speed or high pressure applications.

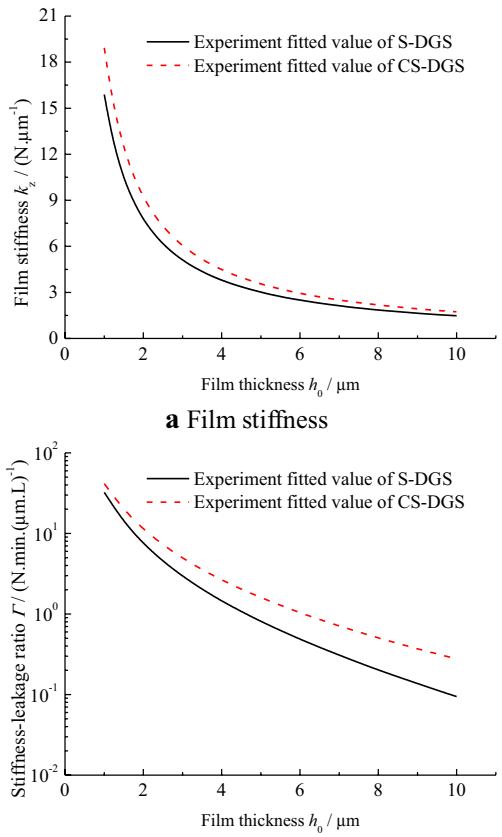

a Film stiffness

b Stiffness-leakage ratio

Figure 14 Comparison of experiment fitted value of film stiffness and stiffness-leakage ratio of S-DGS and CS-DGS

(3) The bionic CS-DGS is a type of hydrodynamic seal for its significant hydrodynamic force generated under high-speed conditions. The leakage and stiffness characteristics of bionic CS-DGS are superior to that of common S-DGS under the condition of high-speed and low-pressure.

Authors' Contributions

X-DP was in charge of the whole trial; J-BJ wrote the manuscript; J-YL and YC assisted with sampling and laboratory analyses. All authors have read and approved the final manuscript.

Authors' Information

Jin-Bo Jiang, born in 1989, is currently a post-doctor at *Engineering Research Center of Process Equipment and Its Re-manufacturing of Ministry of Education, Zhejiang University of Technology, China*. He received his PhD degree from *Zhejiang University of Technology, China*, in 2016. His research interests include bionic design of mechanical face seal. Tel: +86-13819450477; E-mail: jinbo_110@163.com.

Xu-Dong Peng, born in 1964, is currently a professor at *Zhejiang University of Technology, China*. He received his PhD degree from *Xi'an Jiaotong University, China*, in 1999. His research interests include fluid seal technology and design method of surface texture. Tel: +86-571-88871503; E-mail: xdpeng@126.com.

Ji-Yun Li, born in 1965, is currently a professor senior engineer at *Zhejiang University of Technology, China*. She received her master degree in China University of Petroleum. E-mail: lijiyun@zjut.edu.cn.

Yuan Chen, born in 1990, is currently a PhD candidate at *Engineering Research Center of Process Equipment and Its Re-manufacturing of Ministry of Education, Zhejiang University of Technology, China*. E-mail: chenyuan_1221@163.com.

Competing Interests

The authors declare no competing financial interests.

Ethics Approval and Consent to Participate

Not applicable.

Funding

Supported by National Natural Science Foundation of China (Grant No. 51575490), National Key Basic Research Development Plan (973 Plan, Grant No. 2014CB046404), Key Program of Zhejiang Provincial Natural Science Fund Project (Grant No. LZ15E050002), and Zhejiang Provincial Natural Science Foundation of Youth Fund (Grant No. LQ17E050008).

Publisher's Note

Received: 3 May 2016 Accepted: 16 March 2018
Published online: 09 April 2018

References

[1] M T C Faria. An efficient finite element procedure for analysis of high-speed spiral groove gas face seals. *ASME Journal of Tribology*, 2001, 123(1): 205–210.
[2] S T Hu, W F Huang, X F Liu, et al. Influence analysis of secondary O-ring seals in dynamic behavior of spiral groove gas face seals. *Chinese Journal of Mechanical Engineering*, 2016, 29(3): 507–514.
[3] X X Ding, J J Lu. Theoretical analysis and experiment on gas film temperature in a spiral groove dry gas seal under high speed and pressure. *International Journal of Heat and Mass Transfer*, 2016, 96: 438–450.
[4] J Xu, X D Peng, S X Bai, et al. Experiment on wear behavior of high pressure gas seal faces. *Chinese Journal of Mechanical Engineering*, 2014, 27(6): 1287–1293.
[5] Z X Liu, M S Wang, Y Zhou, et al. Dynamic coupling correlation of gas film in dry gas seal with spiral groove. *Chinese Journal of Mechanical Engineering*, 2014, 27(4): 853–859.
[6] Y Chen, J B Jiang, X D Peng. Gas film disturbance characteristics analysis of high-speed and high-pressure dry gas seal. *Chinese Journal of Mechanical Engineering*, 2016, 29(6): 1226–1233.
[7] M Zou, I Green. Clearance control of a mechanical face seal. *Tribology Transactions*, 1999, 42(3): 535–540.
[8] N Zirkelback. Parametric study of spiral groove gas face seals. *Tribology Transactions*, 2000, 43(2): 337–343.
[9] Y C Liu, X M Shen, W F Xu, et al. Performance comparison and parametric study on spiral groove gas film face seals. *Science in China Series G: Physics, Mechanics and Astronomy*, 2004, 47(1): 29–36.
[10] X D Peng, J B Jiang, S X Bai, et al. Structural parameter optimization of spiral groove dry gas seal under low or medium pressure. *CIESC Journal*, 2014, 65(11): 4536–4542. (in Chinese)
[11] H Su, R Rahmani, H Rahnejat. Performance evaluation of bidirectional dry gas seals with special groove geometry. *Tribology Transactions*, 2017, 60(1): 58–59.
[12] H Su, R Rahmani, H Rahnejat. Thermohydrodynamics of bidirectional groove dry gas seals with slip flow. *International of Journal of Thermal Sciences*, 2016, 110: 270–284.
[13] S Blasiak, A V Zahorulko. A parametric and dynamic analysis of non-contacting gas face seals with modified surfaces. *Tribology International*, 2016, 94: 126–137.

[14] H Hashimoto, M Ochiai. Optimization of groove geometry for thrust air bearing to maximize bearing stiffness. *ASME Journal of Tribology*, 2008, 130(3): 031101–031111.
[15] H Hashimoto, T Namba. Optimization of groove geometry for a thrust air bearing according to various objective functions. *ASME Journal of Tribology*, 2009, 131(4): 041704.
[16] H Hashimoto, Y Sunami. Robust optimum design of thrust hydrodynamic bearings for hard disk drives. *Applied Mathematics*, 2012, 3(10): 1368–1379.
[17] X D Peng, L L Tan, S E Sheng, et al. Static analysis of a spiral groove dry gas seal with an inner annular groove. *Tribology*, 2008, 28(6): 507–511. (in Chinese)
[18] H P Bloch. Consider dry gas seals for centrifugal compressors. *Hydrocarbon Processing*, 2005, 84(1): 9–10.
[19] E Vanhie. Gas-lubricated mechanical seals for pumps. *Hydrocarbon Processing*, 2001, 80(1): 63.
[20] J B Jiang, X D Peng, S X Bai, et al. Numerical analysis of characteristics of a bionic cluster spiral groove dry gas seal. *Journal of Mechanical Engineering*, 2015, 51(15): 20–26. (in Chinese)
[21] J B Jiang, X D Peng, J Y Li, et al. A comparative study on the performance of typical types of bionic groove dry gas seal based on bird wing. *Journal of Bionic Engineering*, 2016, 13(2): 324–334.
[22] X Q Yu, S He, R L Cai. Frictional characteristics of mechanical seals with a laser-textured seal face. *Journal of Materials Processing Technology*, 2002, 129(1): 463–466.
[23] S X Bai, X D Peng, L Q Bai. Experimental investigation of an inclined ellipse dimpled gas face seal. *Tribology Transactions*, 2012, 55(4): 512–517.